

Singular mass matrices for isogeometric finite element analysis of dynamic contact

Anton Tkachuk^{1*}, Martina Matzen², Radek Kolman³ and Manfred Bischoff¹

Micro Abstract

Usage of standard mass matrices together with implicit time integration leads to temporal oscillations of contact forces and losses/gains of energy at each contact event. Redistribution of the mass from nodes that are potentially coming into contact and removing the term corresponding to contact forces from the predictor of the Newmark method alleviates both problems. In this contribution a mass redistribution for solid isogeometric FE's is presented and results of numerical tests are discussed.

¹Institute for Structural Mechanics, University of Stuttgart, Stuttgart, Germany

²Bornscheuer Drexler Eisele GmbH, Stuttgart, Germany

³Institute of Thermomechanics, The Czech Academy of Sciences, Prague, Czech Republic

*Corresponding author: tkachuk@ibb.uni-stuttgart.de

Introduction

Accurate numerical schemes for impact response is still a challenging and open problem and area of active research. The main issues for implicit time integration schemes are large temporal oscillation of contact forces and losses/gains of energy at each contact event (activation and release from contact). The latter issue can be addressed with modification of the predictor in the Newmark method as proposed in [5, 7]. The former issue can be efficiently resolved for standard Lagrange elements by redistributing mass from contact surface to inner nodes [6] or for thin-walled elements by redistributing mass in neutral line/surface [8, 13]. Recently, spline-based finite elements got substantial attention because of their superior approximation properties for smooth problems and direct connection with data representation in CAD. Thus, the spline-based approximation in the domain can be combined with modified Newmark time discretization and mass modification techniques to get superior results for dynamic contact problems.

The goal of this contribution is to present a method for stabilization of contact forces in impact problems based on singular mass matrices proposed in [9] and to quantify the grid dispersion error introduced by the novel mass matrix.

1 Spatial and temporal discretization

1.1 Redistribution of mass from contact surface to inner nodes

The mass redistribution formulation should fulfill following conditions: zero mass at each contact node, symmetry and positive semi-definiteness of the mass matrix, preservation of the translational mass and mass of consistent mass, simplicity of construction. The motivation for zero mass is reduction of differential index of the underlying semidiscrete differential-algebraic equation system and improved stability of contact algorithm, see details in [6, 8]. Non-symmetric masses is difficult to explain physically and any negative eigenvalue of a mass matrix leads to an unconditionally unstable solution. Keeping the translational mass is necessary for consistency of the method. Finally, usage of the mask of the consistent mass for a modified mass does not require any changes in sparse matrix management inside the code and simplicity of construction keeps the computational cost low. The modified quadrature rule proposed in [6] satisfies these

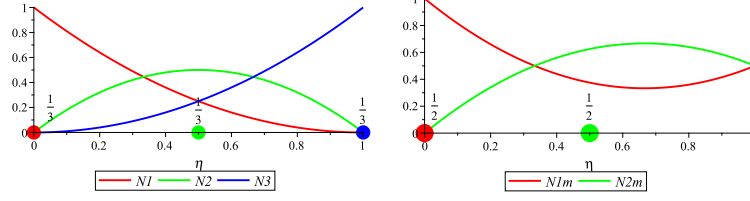


Figure 1. Standard quadratic B-Splines for one element (left) and their modification due to a possible contact at node 3 with $\gamma_s = 0.5$ (right). The lumped masses at the nodes are given by a size of solid circle and a number above.

conditions only for bulk bodies and interpolatory shape functions, e.g. standard Lagrange. The hybrid-mixed methods proposed [8, 13] require that contact nodes possess displacement shape functions being orthogonal to a constant velocity, i.e. $\int_{\Omega} \rho \mathbf{N} \cdot \mathbf{1} dV = 0$. The total positivity property of B-Splines and its common extensions is not compatible with the orthogonality condition. Thus, an alternative method for the B-Spline-based discretization is needed. Here, a formulation proposed in [9, 11] is pursued. The modified mass matrix is computed with modified shape functions \mathbf{N}_m with

$$\mathbf{M}_{m,\text{cons}} = \int_{\Omega} \rho \mathbf{N}_m^T \mathbf{N}_m dV, \quad \mathbf{M}_{m,\text{lumped}} = \int_{\Omega} \rho \mathbf{N}_m dV. \quad (1)$$

The modification of the shape function is done via redistribution of the shape function to neighboring nodes. This redistribution is illustrated on the example of single quadratic element

$$N_1(\eta) = (1 - \eta)^2, \quad N_{1,m}(\eta) = N_1(\eta) + \gamma_s N_3(\eta) \quad (2)$$

$$N_2(\eta) = (1 - \eta)^2, \quad N_{2,m}(\eta) = N_2(\eta) + (1 - \gamma_s) N_3(\eta), \quad (3)$$

$$N_3(\eta) = \eta^2, \quad N_{3,m}(\eta) = 0, \quad (4)$$

where a contact at the node associated with the shape function N_3 is expected. The shape functions are also shown on Figure 1. Such a redistribution preserves the translational mass and fulfills the rest of the conditions on the mass matrix. Equal redistribution with $\gamma_s = 0.5$ is used for quadratic B-Spline/NURBS functions everywhere below.

External and internal forces ($\mathbf{f}^{\text{ext}}, \mathbf{f}^{\text{int}}$) are obtained with standard finite element procedure. The point-to-segment contact formulation is used herein [9] which results in a contact residual \mathbf{f}^c . Finally, we arrive to the semidiscrete equation of motion

$$\mathbf{M} \ddot{\mathbf{U}} = \mathbf{f}^{\text{ext}} - \mathbf{f}^{\text{int}} - \mathbf{f}^c, \quad (5)$$

where \mathbf{M} is some mass matrix, \mathbf{U} is the displacement vector and $(\ddot{\cdot})$ is second derivative in time.

1.2 Modified Newmark integration

In this subsection time integration schemes for regular and singular mass matrices are presented. The former is the contact modified formulation of Kane et al. [7], which is shortly summarized for regular mass matrix. The latter is adjustment of the same formulation of Kane et al. [7] to singular mass matrices. For simplicity, a damping forces and corresponding terms are omitted.

The modified Newmark method is based on an additive split of the acceleration vector in contact and non-contact parts

$$\ddot{\mathbf{U}} = \ddot{\mathbf{U}}^{\text{int}} + \ddot{\mathbf{U}}^c, \quad \mathbf{M} \ddot{\mathbf{U}}^{\text{int}} = \mathbf{f}^{\text{ext}} - \mathbf{f}^{\text{int}}, \quad \mathbf{M} \ddot{\mathbf{U}}^c = -\mathbf{f}^c, \quad (6)$$

denoted with $(\cdot)^c$ and $(\cdot)^{\text{int}}$, respectively. The modified corrector treats the contact forces in pure implicit manner

$$\mathbf{U}_{n+1} = \tilde{\mathbf{U}}_{n+1} + \Delta t^2 \beta \ddot{\mathbf{U}}_{n+1}^{\text{int}} + \frac{1}{2} \Delta t^2 \ddot{\mathbf{U}}_{n+1}^c, \quad \dot{\mathbf{U}}_{n+1} = \dot{\tilde{\mathbf{U}}}_{n+1} + \Delta t \gamma \ddot{\mathbf{U}}_{n+1}^{\text{int}} + \Delta t \ddot{\mathbf{U}}_{n+1}^c, \quad (7)$$

with a corresponding modified predictor

$$\tilde{\mathbf{U}}_{n+1} = \mathbf{U}_n + \Delta t \dot{\mathbf{U}}_n + \frac{1}{2} \Delta t^2 (1 - 2\beta) \ddot{\mathbf{U}}_n^{\text{int}}, \quad \dot{\tilde{\mathbf{U}}}_{n+1} = \dot{\mathbf{U}}_n + \Delta t (1 - \gamma) \ddot{\mathbf{U}}_n^{\text{int}}, \quad (8)$$

where β and γ are parameters of Newmark method and Δt is the time step. Substitution of the corrector in the equilibrium yields the following implicit equation for $\beta > 0$

$$\frac{1}{\beta \Delta t^2} \mathbf{M} (\mathbf{U}_{n+1} - \tilde{\mathbf{U}}_{n+1}) = \mathbf{f}_{n+1}^{\text{ext}} - \mathbf{f}_{n+1}^{\text{int}} - \frac{1}{2\beta} \mathbf{f}_{n+1}^{\text{c}} \quad (9)$$

with a linearization with respect to displacement \mathbf{U}_{n+1}

$$\left(\frac{1}{\beta \Delta t^2} \mathbf{M} + \mathbf{K}_T + \frac{1}{2\beta} \mathbf{K}_c \right) \Delta \mathbf{U}_{n+1} = \mathbf{f}_{n+1}^{\text{ext}} - \mathbf{f}_{n+1}^{\text{int}} - \mathbf{f}_{n+1}^{\text{kin}} - \frac{1}{2\beta} \mathbf{f}_{n+1}^{\text{c}}. \quad (10)$$

Here, $\mathbf{K}_T = d\mathbf{f}_{n+1}^{\text{int}}/d\mathbf{U}_{n+1}$ is the tangent stiffness matrix, $\mathbf{K}_c = d\mathbf{f}_{n+1}^{\text{c}}/d\mathbf{U}_{n+1}$ is the contact stiffness and $\mathbf{f}_{n+1}^{\text{kin}} = \mathbf{M}\ddot{\mathbf{U}}_{n+1}/\beta\Delta t^2$ is the part of the residual due to the inertia forces. This time integration is strictly dissipative for the regular mass matrices as proven in Kane et al. [7]. However, the total loss of the total energy can be unacceptable as it shown in the example below.

In case of singular mass matrix with zero masses at contact nodes equation $\mathbf{M}\ddot{\mathbf{U}}^{\text{c}} = -\mathbf{f}^{\text{c}}$ is inconsistent because non-zero components of contact force vectors correspond to zero rows of the mass matrix. Therefore a split of the global vectors in inner and contact nodes must be done and different predictor and corrector formulas are valid for corresponding DOF's. Subvectors corresponding to inner and contact nodes are denoted by superscripts $(\cdot)^{\text{i}}$ and $(\cdot)^{\text{c}}$, respectively. Thus, the equilibrium equation for inner and contact nodes at time t_{n+1} reads

$$\frac{1}{\beta \Delta t^2} \mathbf{M}^{\text{i}} (\mathbf{U}_{n+1}^{\text{i}} - \tilde{\mathbf{U}}_{n+1}^{\text{i}}) = \mathbf{f}_{n+1}^{\text{ext,i}} - \mathbf{f}_{n+1}^{\text{int,i}}, \quad (11)$$

$$\mathbf{0} = \mathbf{f}_{n+1}^{\text{ext,c}} - \mathbf{f}_{n+1}^{\text{int,c}} - \mathbf{f}_{n+1}^{\text{c}}. \quad (12)$$

The linearization of these equation can be performed as before.

2 Analytical grid dispersion analysis of Rayleigh-Lamb waves

Accuracy of a spatial semi-discretization for transient problems can be studied using the grid dispersion analysis (GDA). This analysis provides relation between the frequency of discretized propagating wave ω^h and the wave vector \mathbf{k} referred here as dispersion relation. The difference between the discrete and a known analytical dispersion relations indicates the error of the spatial discretization. GDA was initially applied to study accuracy of finite difference schemes, but it was lately also used for standard and isogeometric finite elements in [10] and [3], respectively. Here, GDA is performed for a thin plate that guides the Rayleigh-Lamb waves. Quadratic B-Splines are used for discretization in thickness and length direction. Both consistent and singular mass matrix presented above are considered.

Rayleigh-Lamb waves have complicated non-linear dispersion relation with multiple symmetric and anti-symmetric branches [12]. Unfortunately, an explicit form for the dispersion relation does not exist. Rayleigh-Lamb frequency equation is an implicit form of the dispersion relation and it reads

$$\frac{\tan(qh)}{\tan(ph)} = -\frac{4k^2 pq}{(p^2 - q^2)^2} \quad (\text{sym. modes}) \quad \frac{\tan(qh)}{\tan(ph)} = -\frac{(p^2 - q^2)^2}{4k^2 pq} \quad (\text{anti-sym. modes}), \quad (13)$$

where $2h$ is the thickness of the plate, $p^2 = \omega^2/c_L^2 - k^2$ and $q^2 = \omega^2/c_T^2 - k^2$. Here, $c_T = \sqrt{E/(2\rho(1+\nu))}$ and $c_L = \sqrt{E(1-\nu)/(\rho(1+\nu)(1-2\nu))}$ are the transverse and the longitudinal wave velocity, respectively. In addition, the wave vector \mathbf{k} reduces to a wavenumber $k = 2\pi/\lambda$

along the only possible wave propagation direction, where λ is the wave length. The highest importance for the impact problems of thin structures has $A0$, $A1$ and $S0$ branches. $A0$ and $A1$ branches correspond to bending and shear dominant branches of a Mindlin plate theory [12] and $S0$ is the compressional wave. Accuracy of $A0$ and $S0$ at long wave approximation (Taylor expansion $k \rightarrow 0$) is studied below. These reference expressions are taken in a dimensionless form from [1] w.r.t. dimensionless frequencies $\Omega = \omega h/c_T$ and wavenumber $\kappa = hk$

$$\Omega_{S0}^2 = \frac{2}{1-\nu}\kappa^2 - \frac{2\nu^2}{3(1-\nu)^3}\kappa^4 + \frac{2\nu^2(7\nu^2 + 10\nu - 6)}{45(1-\nu)^5}\kappa^6 + O(\kappa^8) \quad (14)$$

$$\Omega_{A0}^2 = \frac{2}{3(1-\nu)}\kappa^4 + \frac{2(7\nu - 17)}{45(1-\nu)^2}\kappa^6 + O(\kappa^8). \quad (15)$$

All branches of the discrete dispersion relation are contained in a characteristic equation

$$C(\kappa, \Omega^h) = \det \left(\mathbf{K}_{dyn}(\kappa, \Omega^h) \right) = 0, \quad (16)$$

built for a representative patch of the mesh shown on Figure 2. This characteristic equation contains three symmetric and three asymmetric branches for consistent mass matrix and two symmetric and two asymmetric branches singular mass matrix, which can be visualized using numerical root finding, e.g. with help of computer algebra system *Maple*, see Figure 2. However, direct computation of the order of accuracy from equation (16) using implicit function theorem is troublesome. Here, we follow the method of power balance, see [1]. The analytical dispersion relation for consistent mass matrix and quadratic IGA with three control points per thickness is obtained as

$$\Omega_{S0}^{CMM,2} = \frac{2}{1-\nu}\kappa^2 - \frac{2\nu^2}{3(1-\nu)^3}\kappa^4 - \frac{2\nu^6 - 18\nu^5 + \nu^4 + 10\nu^2 - 6\nu + 1}{45(1-\nu)^5(1-2\nu)}\kappa^6 + O(\kappa^8) \quad (17)$$

$$\Omega_{A0}^{CMM,2} = \frac{2}{3(1-\nu)}\kappa^4 + \frac{2\nu^2 + 8\nu - 29}{45(1-\nu)^2}\kappa^6 + O(\kappa^8). \quad (18)$$

The analytical dispersion relation for singular mass matrices and quadratic IGA with three control points per thickness is obtained as

$$\Omega_{S0}^{sing,2} = \frac{2}{1-\nu}\kappa^2 - \frac{2(41\nu^2 - 10\nu - 35)}{45(1-\nu)^3}\kappa^4 + O(\kappa^6) \quad (19)$$

$$\Omega_{A0}^{sing,2} = \frac{2}{3(1-\nu)}\kappa^4 + \frac{2\nu^2 - 16\nu - 25}{45(1-\nu)^2}\kappa^6 + O(\kappa^8). \quad (20)$$

Comparison of the Taylor series for the dispersion (15) and (20) shows that the main term of dispersion relation for the bending branch ($A0$) is preserved despite mass modification. The main term of error in the branch ($A0$) is of 6th order for CMM (18) and for the singular mass (20). The advantage of CMM over the singular mass shows only in the volumetric branch ($S0$) yielding 4th vs. 2nd order of accuracy

3 Numerical example

Consider a transient contact problem described on Figure 3. A quarter of an elastic thin ring bounces onto a rigid planar frictionless obstacle. After several contacts events the ring re-bounce keeping the total energy of the system. The initial velocity of the ring $v_0 = 0.5$ m/s is about 3.9 % of shear wave velocity. Therefore, substantial deformation of the ring is expected. Moreover, the ring undergoes rotation of almost 90° due to the series of the impacts. The focus of the benchmark is to check smoothness of the contact forces, energy preservation and general robustness of the algorithm. Here, the results obtained with standard lumped mass are compared with singular mass matrix given in above.

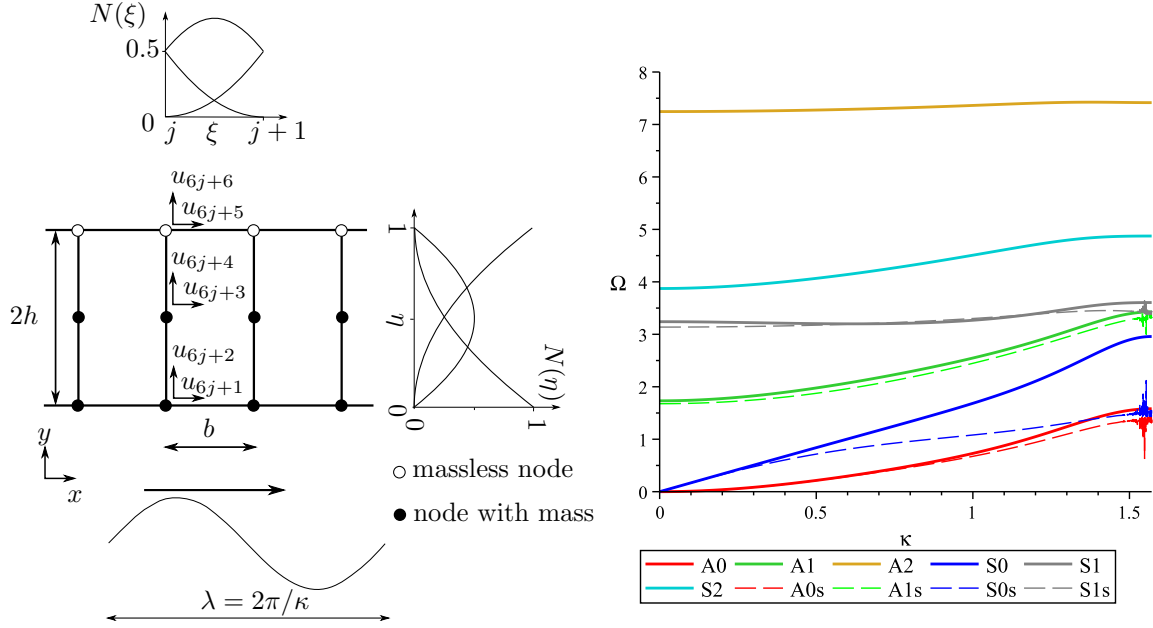


Figure 2. Setup for analytical dispersion analysis in a plate discretized with quadratic B-Spline shape functions (left) and comparison of dispersion relations for CMM and singular mass matrix for aspect ratio $h/b = 2$ (right). Results for singular mass are marked with 's'.

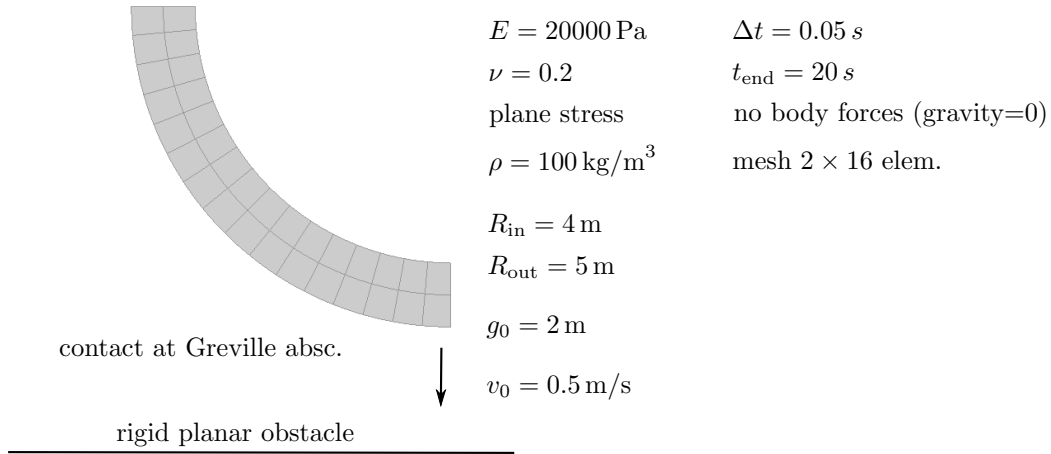


Figure 3. Setup for the transient benchmark.

Contact modified Newmark algorithm with constant time step 0.05 s and parameters $\beta = 0.25$ and $\gamma = 0.5$ is used. The mesh is obtained from single quadratic NURBS patch via standard uniform knot insertion algorithm. Elastic St.Venant-Kirchhoff material with plane stress assumption is used. Contact is enforced with Lagrange multipliers method at Greville abscissa. Alternatively, uniform, Botella [2] or Chebyshev-Demko [4] can be used, but the numerical evidences show no advantages of using them in comparison with Greville abscissa [9].

The example is computed in in-house code *NumPro*, see details of the implementation in [9,11]. The drop tolerance for the total residual is chosen to be $1.0 \cdot 10^{-8}$. Full Gauss quadrature (3×3) is used for the internal force vector and mass matrix calculations.

The results of simulation are presented on Figure 4. The history of the contact force with standard mass shows higher spikes and more oscillations. Combination of the modified Newmark algorithm and lumped mass matrix yields reduction of the total energy by 9.5 % after re-bounce whereas the same time integration with the singular mass yields energy reduction by 0.097 %.

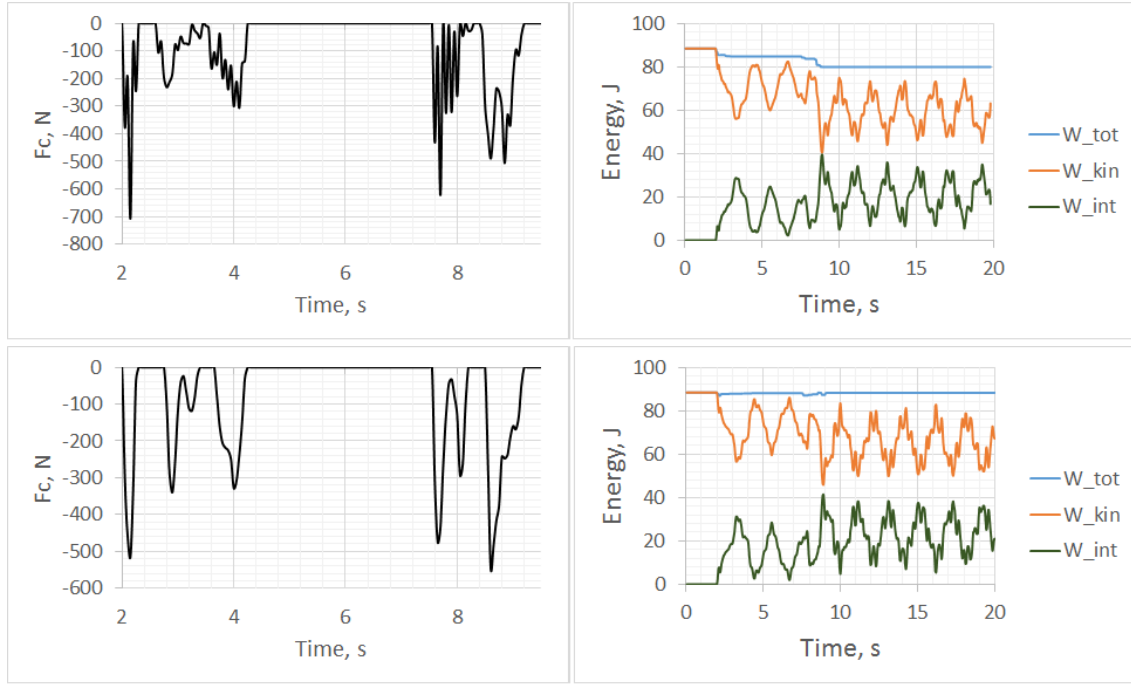


Figure 4. Evolution of contact force and total energy with lumped mass matrix (above) and singular mass matrix (below).

Conclusions

Singular mass matrices for isogeometric finite elements improve energy preservation and robustness of analysis of dynamic contact problems. The algorithm with mass redistribution yields symmetric and positive semi-definite mass matrices that preserve translational mass of structure, which are minimal conditions for consistency. The grid dispersion analysis of a thin plate discretized with the modified mass shows that this mass redistribution does not significantly affect the bending dominated branch. This explains why a transient benchmark with a ring modeled with few isogeometric element in thickness and the singular mass shows high accuracy of the solution.

The study here was limited to one value of the mass redistribution parameter $\gamma_c = 0.5$, constant time step and bi-quadratic fully integrated B-Splines/NURBS elements. Further investigation of the mass redistribution for different values of γ_c , bi-cubic B-Splines/NURBS and other integration strategies can be done.

Acknowledgements

The work was supported by the the bilateral mobility project No. DAAD-16-12 and Projekt-ID 57219898 funded via DAAD from Federal Ministry of Education and Research. The work of R. Kolman was also supported by the Centre of Excellence for Nonlinear Dynamic Behaviour of Advanced Materials in Engineering CZ.02.1.01/0.0/0.0/15_003/0000493 (Excellent Research Teams) in the framework of Operational Programme Research, Development and Education.

References

- [1] F. A. Amirkulova. *Dispersion relations for elastic waves in plates and rods*. PhD thesis, Rutgers, The State University of New Jersey, 2011.
- [2] O. Botella. On a collocation B-spline method for the solution of the Navier-Stokes equations. *Computers & fluids*, 31(4):397–420, 2002.

- [3] J. Cottrell, A. Reali, Y. Bazilevs, and T. Hughes. Isogeometric analysis of structural vibrations. *Computer Methods in Applied Mechanics and Engineering*, 195:5257–5296, 2006.
- [4] S. Demko. On the existence of interpolating projections onto spline spaces. *Journal of approximation theory*, 43(2):151–156, 1985.
- [5] P. Deuffhard, R. Krause, and S. Ertel. A contact-stabilized Newmark method for dynamical contact problems. *International Journal for Numerical Methods in Engineering*, 73(9):1274–1290, 2008.
- [6] C. Hager, S. Hübner, and B. I. Wohlmuth. A stable energy-conserving approach for frictional contact problems based on quadrature formulas. *International Journal for Numerical Methods in Engineering*, 73(2):205–225, 2008.
- [7] C. Kane, E. Repetto, M. Ortiz, and J. E. Marsden. Finite element analysis of nonsmooth contact. *Computer Methods in Applied Mechanics and Engineering*, 180:1–26, Nov. 1999.
- [8] H. B. Khenous, P. Laborde, and Y. Renard. Mass redistribution method for finite element contact problems in elastodynamics. *European Journal of Mechanics - A/Solids*, 27(5):918–932, Sept. 2008.
- [9] M. E. Matzen. *Isogeometrische Modellierung und Diskretisierung von Kontaktproblemen*. PhD thesis, Institut für Baustatik und Baudynamik, Universität Stuttgart, Stuttgart, 2015.
- [10] R. Mullen and T. Belytschko. Dispersion analysis of finite element semidiscretizations of the two-dimensional wave equation. *International Journal for Numerical Methods in Engineering*, 18(1):11–29, 1982.
- [11] J. Postupka. Isogeometrische, dynamische kontaktanalyse (15/02). Master’s thesis, Institut für Baustatik und Baudynamik, Universität Stuttgart, Stuttgart, 2015.
- [12] J. L. Rose. *Ultrasonic waves in solid media*. Cambridge university press, 2004.
- [13] A. Tkachuk, B. Wohlmuth, and M. Bischoff. Hybrid-mixed discretization of elasto-dynamic contact problems using consistent singular mass matrices. *International Journal for Numerical Methods in Engineering*, 94(5):473–493, 2013.